Roll control of a MALE UAV using the adaptive torsion wing

R. M. Ajaj
r.m.ajaj@swansea.ac.uk
M. I. Friswell, W. G. Dettmer, A. T. Isikveren and G. Allegri
College of Engineering
Swansea University
Swansea, UK

ABSTRACT

This paper assesses the feasibility of the Adaptive Torsion Wing (ATW) concept to replace conventional ailerons and enhance the manoeuvrability of a MALE UAV. The ATW concept is a thin-walled closed section two-spar wingbox whose torsional stiffness can be adjusted through the chord-wise position of the front and rear spar webs. The reduction in torsional stiffness allows external aerodynamic loads to induce aeroelastic twist that can be used as a function of the flight conditions to obtain a desired roll control authority. Modelling of the concept was performed using a conceptual design tool developed in MATLAB™. The variation of structural figures of merit are evaluated and discussed. Finally, an MDO study was performed to have in-depth assessments of the potential benefits of the ATW in replacing ailerons and providing sufficient roll control.

NOMENCLATURE

a	Lift-curve slope
$\hat{a}$	Normalised pitch axis location with respect to half chord ($\hat{a} = -1$ leading edge, $\hat{a} = 1$ trailing edge)
A	Enclosed area
[**A**]	Aerodynamic inertia matrix
[**B**]	Aerodynamic damping matrix
c	Wing chord
[**C**]	Structural damping matrix
[**D**]	Aerodynamic stiffness matrix
ds	Infinitesimal segment along the perimeter of the closed section
G	Shear modulus

Paper No. 3809. Manuscript received 10 October 2011, revised version received 13 June 2012, accepted 29 June 2012.

J	Torsion constant
[**K**]	Stiffness matrix
l	Wing semi-span
L'	Lift per unit span
L	Rolling moment
[**M**]	Inertia matrix
M'	pitching moment per unit span
N	Yawing moment
t	Wall thickness
V	Airspeed
w	Plunge displacement at shear centre
x	Web position as percentage of the wingbox chord (%)
{**q**}	Vector of degrees of freedom
θ	Twist angle
ρ	Air density

Subscripts

d	Divergence
dd	Dive
f	Flutter

1.0 INTRODUCTION

Active Aeroelastic Structures (AAS) are a subset of adaptive structures that allow significant performance improvements by manipulating the aerodynamic profile of a lifting surface, without the need for large planform modifications that typically require complex and heavy mechanisms. Traditional design strategies avoided flexible wing designs to prevent aeroelastic problems and maintain structural integrity over a wide range of flight conditions. This resulted in significant weight penalties, typically ranging from 2% to 5% of the structural wing weight[1] which penalised the aircraft performance and increased fuel burn. On the contrary, AAS exploit the aeroelastic deformations due to structural flexibility in a beneficial manner in order to enhance flight performance. The authority of conventional control surfaces can also be augmented via AAS, thus leading to flexible and lighter wing designs. Since AAS use the external aerodynamic loads to deform and maintain their displaced shape, this may reduce the actuation energy requirements associated with these structures.

AAS seems to be a very attractive and promising alternative to achieve morphing capabilities. Recently, the use of AAS to enhance flight performance and enhance control authority and stealth characteristics for air-vehicles has been under thorough investigation in a number of research programs and projects across the world. In the United States of America, both the Active Flexible Wing (AFW) program[2] and the Active Aeroelastic Wing (AAW) program[3,4] investigated the use of flexible wing structures coupled with leading and trailing edge control surfaces. The structural deformations of an advanced fighter wing were manipulated in order to eliminate aileron reversal problems at large dynamic pressures and to maximise the rolling performance according to design intent without using the horizontal tail to augment roll performance. Furthermore, Griffin *et al*[5] investigated the use of a smart spar concept to vary the torsional stiffness and to control the aeroelastic behaviour of a representative wing; this design concept

also aimed to enhance the roll rate of high performance aircraft at high dynamic pressures. The solution proposed was based on the simultaneous actuation of control surfaces and the modification of the wing torsional stiffness using the aforementioned smart spar concept. The latter has a web that can either transfer shear between the upper and lower spar caps or disable such load transmission mechanism. This is achieved by allowing the smart spar to move from a reference position along the leading edge to a diagonal arrangement where the front caps at the wing root are connected to the aft most ones at the wing tips. Similarly, Chen *et al*[6] developed the Variable Stiffness Spar (VSS) concept to vary the torsional stiffness of the wing and again enhance the roll performance. Their VSS concept consisted of a segmented spar having articulated joints at the connections with the wing ribs and an electrical actuator capable of rotating the spar through 90°. In the horizontal position, the segments of the spar are uncoupled and the spar offers no bending stiffness. In the vertical position, the segments join completely and the spar provides the maximum torsional and bending stiffness. The concept allows the stiffness and aeroelastic deformations of the wing to be controlled depending on the flight conditions.

Nam *et al*[7] took the VSS solution a step forward and developed the torsion-free wing concept. This aimed to attain a post-reversal aeroelastic amplification of wing twist. The primary structure of the torsion free wing consists of two main parts. The first is a narrow wingbox tightly attached to the upper and lower wing skin in order to provide the basic wing torsional stiffness. The second part consists of two variable stiffness spars placed near the leading and trailing edges, passing through all of the ribs. Nam *et al* demonstrated that the torsion-free wing can provide significant aeroelastic amplification, leading to an increase in roll-rate between 8% and 48% over the baseline performance in the worst possible flight conditions. Florance *et al*[8] investigated the use of the VSS concept to exploit the wing flexibility and to improve the aerodynamic performance of the vehicle. Their wing incorporated a spar with a rectangular cross-section that runs from the wing root up to 58% of the overall wing semi-span. The spar is used to change the wing bending and torsional stiffness as it rotates between vertical and horizontal positions.

In Europe, the Active Aeroelastic Aircraft Structures (3AS) research project[9-11] which involved a consortium of 15 European partners in the aerospace industry and was partially funded by the European Community, focused on developing active aeroelastic design concepts through exploiting structural flexibility in a beneficial manner. The final aim was to improve the aircraft aerodynamic efficiency. One of the novel concepts proposed was the All-Moving Vertical Tail (AMVT) with a variable torsional stiffness attachment[12,13]. The AMVT concept achieved a smaller and lighter fin while maintaining stability and rudder effectiveness for a wide range of airspeeds. The AMVT employs a single attachment and the position of the attachment can be adjusted in the chord-wise direction relative to the position of the centre of pressure to achieve aeroelastic effectiveness above unity[12]. Furthermore, the 3AS project investigated a variety of variable stiffness attachments and mechanisms for the AMVT concept including a pneumatic device developed at the University of Manchester[13]. As part of the 3AS project, Cooper *et al*[14-16] investigated two active aeroelastic structure concepts that modify the static aeroelastic twist of the wing by modifying its internal structure. The first concept exploited the chord-wise translation of an intermediate spar in a three spars wingbox in order to vary its torsional stiffness and the position of the shear centre. The second concept was similar to the VSS concept where rotating spars are employed to vary the torsional and bending stiffness as well as the shear centre positions. Prototypes of such concepts were built and tested in the wind tunnel to examine their behaviour under aerodynamic loadings.

2.0 THE ADAPTIVE TORSION WING (ATW)

The ATW concept is a thin-walled closed section wingbox (Fig. 1(a)) whose torsional stiffness can be adjusted through the relative position of the front and rear spar webs. The torsional stiffness (GJ) for a thin-walled closed section can be estimated from the Bredt-Batho equation as:

$$GJ = \frac{4GA^2}{\oint \frac{\mathrm{d}s}{t}} \quad \ldots (1)$$

where G is the shear modulus, J is the torsion constant, A is the enclosed area, t is the wall thickness, and ds is an infinitesimal segment along the perimeter. If a single material is used in the wingbox, the resulting torsional stiffness depends mainly on the square of the enclosed area for a given wall thickness; therefore the torsional stiffness of the section can be altered by varying the position of the front spar web, the rear spar web, or both, to change the enclosed area, as shown in Fig. 1(a). The connecting ribs shown in Fig. 1(a) are assumed to maintain the load transfer between the spars and the covers to maintain a closed-section wingbox (for Equation (1) to be valid). As the webs position is altered the spanwise bending stiffness remains constant while the chordwise bending stiffness varies accordingly. The change in web positions (Figs 1(b) and 1(c)), results in two components of torsional stiffness; the first component is due to the closed section while the second comes from the skin/web segments belonging to the open section(s). The analysis in this paper accounts only for the closed-section component, because the torsional stiffness associated with the open section segments is several orders of magnitude smaller.

In terms of potential control applications, the ATW can be employed to:

- increase lift coefficient (act as flaps or slats)
- replace or augment the performance of conventional ailerons
- enhance the stealth characteristics of the aircraft; and
- provide active load alleviation due to gust and manoeuvre loads

The ATW wingbox concept allows the static aeroelastic shape of the wing to be controlled to enhance flight control depending on the instantaneous flight conditions and mission objectives.

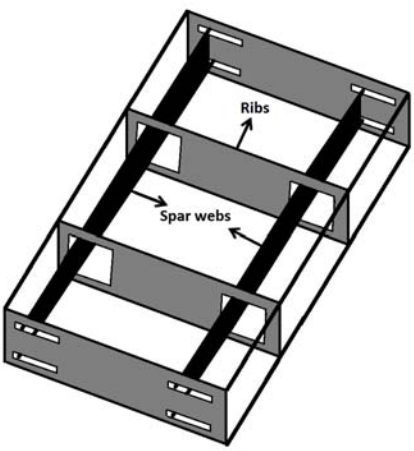

(a) The Adaptive Torsion Wingbox

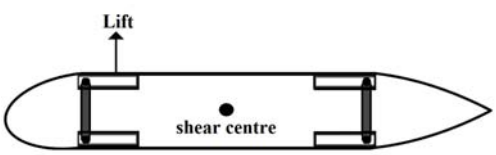

(b) Maximum torsional stiffness

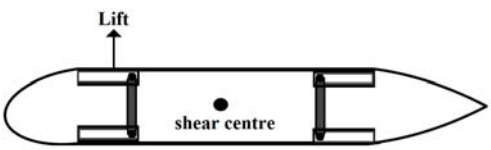

(c) Minimum torsional stiffness positions

Figure 1. A conceptual sketch of the Adaptive Torsion Wing concept.

The spar webs are connected to the hollowed spar flanges through connecting shafts. In this paper, it is assumed that the structural combination behaves as an ideal structure. For practical applications, the choice between moving the front web, the rear web, or both must take into account other structural design considerations such as the change in shear centre position due to the web shift, as this can have a significant impact on the behaviour of the structure. Furthermore, the choice between the three options must account for the increase in system's weight (actuation), structural weight and complexity.

3.0 CONCEPTUAL MODELLING

A conceptual design tool suite was employed to assess the feasibility of the concept and to define potential areas of applications. The tool models the ATW as a quasi-static aeroelastic problem, where the changes in web positions alter the torsional stiffness of the wing and this leads to additional twist deformation induced by the instantaneous aerodynamic loads. The tool consists of the Tornado Vortex Lattice Method (TVLM), a Structural and Finite Element (FE) model, and unsteady flutter and divergence checks, as shown in Fig. 2.

To simplify the analysis and the modelling process, a representative untapered, unswept rectangular wing of a UAV is considered. The conventional two spar wingbox, made entirely from Aluminium 2024-T3 alloy, is replaced with an Aluminium 2024-T3 alloy ATW wing-box concept where the front spar web located originally at 20% of the local wing chord, and the rear spar web located originally at 70% of the local wing chord are allowed to translate inward towards each other up a to maximum displacement equal to 25% of the wingbox chord. The specifications of the UAV are listed in Table 1.

Table 1
The UAV's specifications

UAV specifications	Values
Wing area	$22{\cdot}44\text{m}^2$
MTOW	800kg
Cruise speed	60ms^{-1}
Design dive speed	$\approx 75\text{ms}^{-1}$
Span	12m
Chord	1·87m

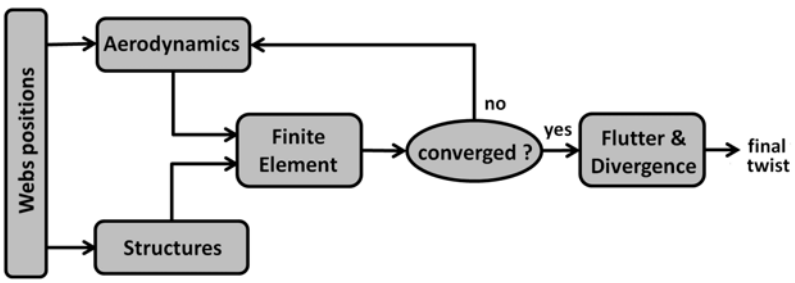

Figure 2. Flowchart for the quasi-static suite.

3.1 Aerodynamics

The Tornado Vortex Lattice Method (TVLM)[20,21] was used for the aerodynamic predictions. Tornado is a linear aerodynamics code, and thus it discounts wing thickness and viscous effects. These limitations imply that Tornado can only be used for angles of attack up to 8-10° for slender wings. Linear aerodynamic theory is still nevertheless very useful as most aircraft typically operate within the linear region (operating lift coefficients at reference speeds) in cruise, as well as both take-off and landing phases. These are the flight stages in which this research and analysis has been undertaken. The representative UAV considered is similar to the BAE Systems Herti UAV. Figure 3 shows the wing (and ailerons) and empennage of the baseline UAV built in Tornado. A convergence study was undertaken to select the optimum spanwise mesh. This study shows that 10 spanwise panels are enough to model the aerodynamic loads on the wing when the aeroelastic deformations are neglected. However, the study showed that 60 spanwise panels are required to model the aerodynamic loads when aeroelastic deformations are considered, yielding a relative error of 0·5% in the lift force. Therefore, in this analysis, 4 chordwise panels and 60 spanwise panels with a cosine distribution are used per wing semi-span. The fuselage contribution to parasitic drag is accounted for by assuming an equivalent cylinder model.

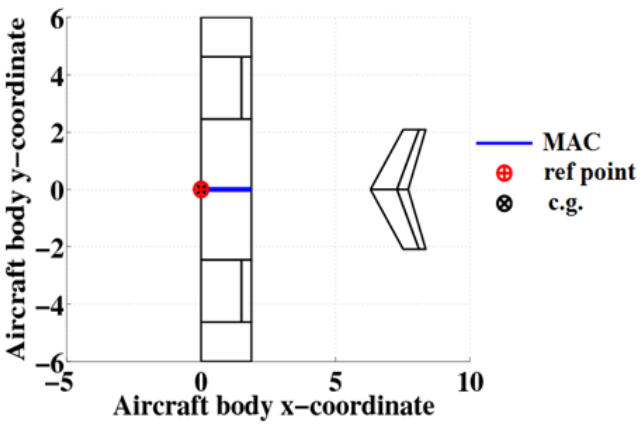

Figure 3. The geometry of the UAV in Tornado.

3.2 Structures and FE model

The wingbox is modelled as a thin-wall Euler-Bernoulli beam with torsion. It is discretised into finite elements, and the conceptual sizing of its various components is performed locally along the span using an ultimate load factor and a safety factor. The structural properties of the elements are then computed. Throughout the sizing process, the webs are assumed to be located at their original positions corresponding to the maximum torsional stiffness, as shown in Fig. 1(b). The wingbox is assumed to be made of Aluminium 2024-T3. An ultimate load factor of 6g and a safety factor of 1·5 are used in the wingbox sizing. A convergence study showed that 12 structural elements are required. Therefore the wingbox is discretised into 12 equal elements, each having a length of 0·5m. After wingbox sizing, an in-house 1-D FE model rearranges the spanwise aerodynamic loads into equivalent loads at the nodes of each of the 12 elements. The inertia and stiffness matrices for every element are computed and transformed from their local coordinates to the wing coordinates (global) and then they are assembled to give the wing inertia and stiffness

matrices [**M**] and [**K**] respectively. This analysis neglects the structural damping terms. Six degrees of freedom are considered per node. The nodal deflections are then computed and fed back into Tornado to modify the wing vortex lattice geometry and to generate new aerodynamic loads. This process continues until the aeroelastic loop converges and equilibrium between aerodynamic loads and wing deflection is established.

3.3 Shear centre position

A design module to estimate the shear centre position for different web positions has been developed. The wingbox is modelled as an equivalent rectangular cross-section as shown in Fig. 4. The connecting ribs are assumed to maintain the load transfer between the spars and the covers and hence the ATW can be approximated as a closed continuous section. The shear centre is defined as the point in the cross-section through which shear loads produce no twisting[22]. Therefore its position is estimated by equating the moment produced by the overall shear force acting on the cross-section and the total moment produced by the shear forces in the individual members of the wingbox (equivalent skins and webs). The individual shear forces in each member are obtained by integrating the shear flow in those members.

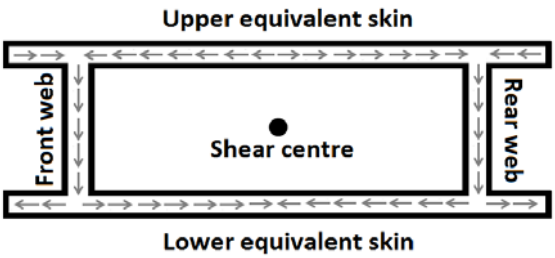

Figure 4. The shear flow in an equivalent wingbox section.

3.4 Flutter and divergence

Flutter (bending-torsion) and divergence checks are also included using the the finite element model coupled with Theodorsen's unsteady aerodynamic theory[19,23,24]. The wing's stiffness and inertia matrices, are extracted from the FE model and reduced into 3 degrees of freedom per node. These degrees of freedom correspond to plunge, pitch (twist), and bending rotation. For unsteady aerodynamics, the lift force per unit span (L') on the aerodynamic centre and the pitching moment (M') per unit span at the elastic axis can be expressed as:

$$L' = \frac{\pi\rho c^2}{4}\left[-\ddot{w} + V\dot{\theta} - \hat{a}\frac{c}{2}\ddot{\theta}\right] + \pi\rho V c C(k)\left[-\dot{w} + V\theta + \frac{c}{2}\left(\frac{1}{2} - \hat{a}\right)\dot{\theta}\right] \quad \ldots (2)$$

$$M' = \frac{\pi\rho c^2}{4}\left[-\hat{a}\frac{c}{2}\ddot{w} - V\frac{c}{2}\left(\frac{1}{2} - \hat{a}\right)\dot{\theta} - \frac{c^2}{4}\left(\frac{1}{8} + \hat{a}^2\right)\ddot{\theta}\right] + \pi\rho V c\frac{c}{2}\left(\frac{1}{2} + \hat{a}\right)C(k)\left[-\dot{w} + V\theta + \frac{c}{2}\left(\frac{1}{2} - \hat{a}\right)\dot{\theta}\right] \quad \ldots (3)$$

where ρ is the air density, V is the airspeed, a normalised pitch axis location with respect to half chord, c is the wing chord, w is vertical the plunge displacement, θ is the pitch displacement (twist), and $C(k)$ is Theodorsen's transfer function. In order to obtain the lift and moment per unit span

in the time domain, a low-dimensional state-space representation of the classical unsteady aerodynamic model of Theodorsen was employed. This low dimensional representation employs a Padé approximation of Theodorsen's transfer function. Ajaj *et al*[19] provide more details about reduced order, state-space representation of the classical unsteady aerodynamics. Then the nodal forces and moments are obtained by integrating the lift and pitching moment per unit span over half the length of each node's adjacent elements. The governing equations of motion of the wing can be arranged as:

$$([\mathbf{M}] - [\mathbf{A}])\{\ddot{\mathbf{q}}\} + ([\mathbf{C}] - [\mathbf{B}])\{\dot{\mathbf{q}}\} + ([\mathbf{K}] - [\mathbf{D}])\{\mathbf{q}\} = 0 \quad \ldots (4)$$

where [**A**] is the aerodynamic inertia matrix, [**B**] is the aerodynamic damping matrix, [**D**] is the aerodynamic inertia matrix, [**C**] is the structural damping matrix which is set to zero in this study, and {**q**} is the vector of the degrees of freedom. Then the equations of motion are arranged in state-space form and the flutter and divergence speeds are estimated using the eigenvalues of the system. To obtain the flutter speed, the flight speed is increased gradually until the real part of one of the complex eigenvalues becomes positive. At this point, flutter is initiated and the speed at which this occurs is the flutter speed. Similarly for divergence speed, the damping matrices are set to zero, and the flight speed is increased gradually until one of the real eigenvalues of becomes positive. At this point, divergence is initiated and the speed at which this occurs is the divergence speed.

4.0 FEASIBILITY STUDY

A feasibility study is conducted to study the variation of various structural figures of merit with the chordwise positions of the webs. These figures of merit include the torsional constant, shear centre position, tip twist, wing lift, divergence speed, and flutter speed. These variations are computed using the conceptual design tool and presented in Figs 5 to 10.The analysis in this section was conducted at cruise, where the UAV is flying at 3,050m (10,000ft). with a speed of 60ms^{-1}. All of the results presented in Figs 5-10 are normalised by their corresponding values when the webs are in their original positions (maximum torsional stiffness) as shown in Fig. 1(b). Note that the viewing angle in the figures is varied to provide the reader with the best view of the corresponding surfaces.

As shown in Fig. 5, the variation of the torsion constant (J) is almost linear with different web positions. Both the front and rear webs produce an equal change in the torsion constant, because they have the same influence on the enclosed area. Shifting the front web alone or the rear web

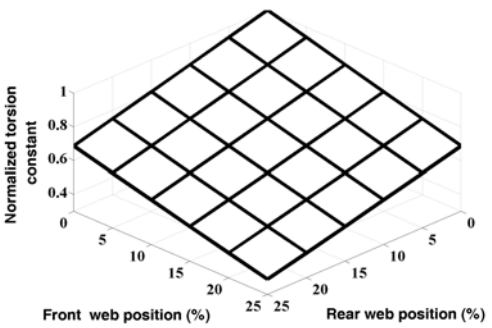

Figure 5. Variation of normalised torsion constant.

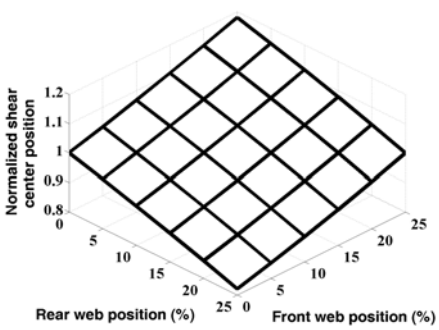

Figure 6. Variation of normalised shear centre position.

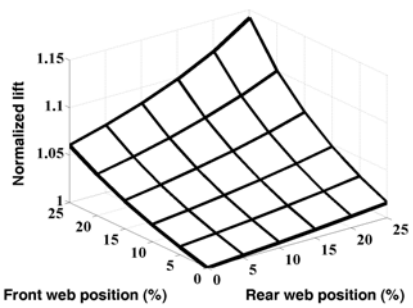

Figure 7. Variation of normalised lift.

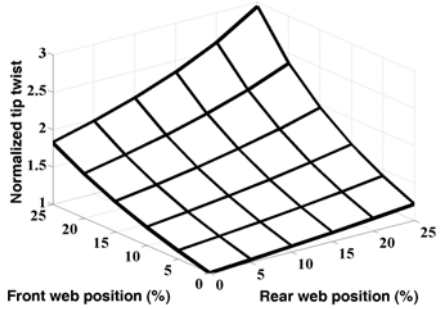

Figure 8. Variation of normalised tip twist.

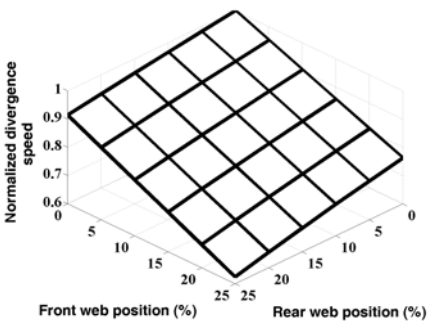

Figure 9. Variation of normalised divergence speed

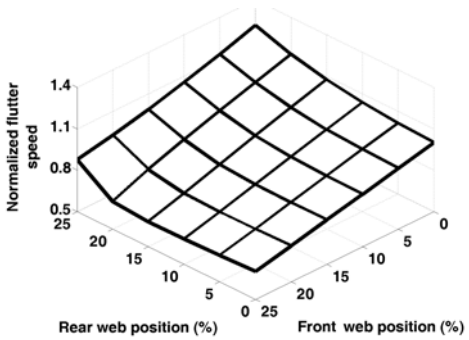

Figure 10. Variation of normalised flutter speed.

alone by 25% of the chord reduces the torsion constant by 32%. Similarly, Fig. 6 presents the variation in the shear centre position with different web positions. The front and rear webs produce an equal change in the shear centre position but in different directions. If the front spar web is shifted back by 25%, then the shear centre is pushed aft by 18% of the wingbox chord; similarly if the rear spar web is moved forward by 25%, then the shear centre is shifted forward again by 18%.

Unlike the torsion constant and the shear centre position, the changes in the front or rear web positions produce different effects on the tip twist and lift force. Figure 7 presents the variation in tip twist with different web positions. The tip twist achieved by moving the front web while keeping the rear fixed, is much higher than that achieved by moving the rear web while keeping the front fixed. The main reason is that moving the front web also pushes the shear centre rearward, so the lift moment arm increases. For instance, shifting the front web by 25% of the chord while keeping the rear fixed in its original position increases the tip twist by 83%. On the other hand, shifting the rear web by 25% while keeping the front web fixed in its original position increases the tip twist by 22%. Figure 8 presents similar results in terms of lift produced by the wing; the total lift is more sensitive to the front spar web shift due to the larger twisting angles attained.

Figure 9 illustrates the variation of divergence speed with different web positions. This is significantly reduced by shifting the front web while keeping the rear web fixed; for instance, shifting the front web by 25% while keeping the rear web at its original position reduces the divergence

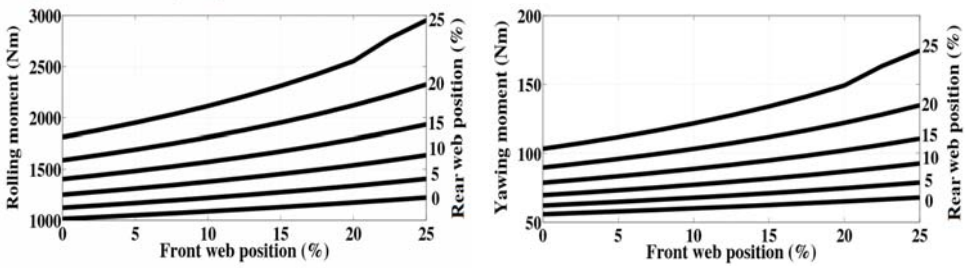

(a) Rolling moment (b) Induced yawing moment

Figure 11. Moments for different web positions.

speed by about 31%. However, shifting the rear web while keeping the front web fixed produces a reduction of 9%. Figure 10 presents the variation of flutter speed with different web positions. As the front web is shifted alone by 25% of the wingbox, the flutter speed drops by 30%, however if the rear web is shifted forward by 25% while keeping the front web fixed, flutter speed increases by 22%. This is because the shear centre shifts forward as the rear web is moved forward, reducing the moment arm and hence increasing the flutter speed.

Figures 5 to 10 indicate that translating the front web while fixing the rear web provides significant increase in lift as well as tip twist. However it reduces the divergence and flutter speeds significantly and limits the use of the ATW concept to low speed flight phases such as take-off and landing. On the other hand, shifting the rear web while keeping the front web in its original position provides a small increase in lift and tip twist but allows control of the flutter and divergence envelopes. Therefore, the choice between translating the front web, rear web, or both depends solely on the application and the loading scenario. Furthermore, it can be concluded from the above figures that a targeted wing deformation (lift or tip twist) can be achieved by different combinations of web positions. Therefore, an optimiser is required to determine the best combination of web positions to maximise the tip twist or lift for a given instantaneous flight condition while minimising the actuation power required.

One of the potential applications of the ATW device is to replace conventional ailerons or to augment their performance. The roll control is achieved by changing the web positions on one side of the wing, resulting in a lift differential and hence generating a rolling moment. Figure 11 illustrates the rolling moment and induced yawing movement generated by altering the web positions on one side of the wing. Shifting the front web rearward by 25% and the rear web forward by 25% on one side of the wing generates a rolling moment of 3kNm and a yawing moment of 175Nm.

6.0 CONTROL OPTIMISATION

The feasibility study showed that significant increase in tip twist and lift can be achieved with the ATW which can be used to augment roll control and agility. In this section, a multidisciplinary design optimisation (MDO) study is performed to have in-depth assessments of the potential benefits of ATW on the UAV level. Stability and control benefits are investigated by operating the ATW on one side of the wing to provide roll control. In the feasibility study above, the ATW was considered to be continuous along the semi-span of the wing and the front web was allowed to shift rearward no more than 25% and the rear web was allowed to shift forward by no more than 25%. On the contrary, in this section each side of the wing is split into morphing partitions from root to tip, and the ATW concept is employed within each partition as shown in Fig. 12. At the ends

of each partition, there are thick connecting ribs that allow the spar webs of each partition to translate independently of the webs of the adjacent partitions. Furthermore, the thick ribs transfer the shear loads between the webs of adjacent partitions and between the webs and the equivalent skins (covers and stringers) to maintain a closed wingbox section and a continuous load path across the various components of the wingbox. A feasibility study showed that 5 partitions and of equal lengths are sufficient to capture the sensitivity of spanwise twist to the web positions in each partition. The number of variables to be controlled increases by splitting each side of the wing into 5 partitions with 2 spars per partition.

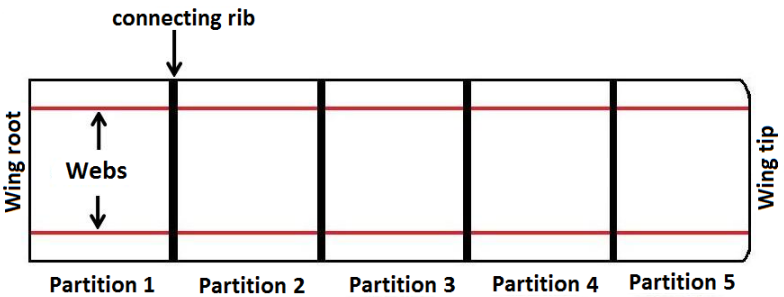

Figure 12. The multi-partition ATW concept without geometric pre-twist.

6.1. MDO Suite

An MDO suite consisting of the Genetic Algorithm (GA) optimiser coupled with conceptual design tool discussed above. The MDO suite belongs to the family of high-end, low-fidelity optimisation tools. A flowchart of the suite is shown in Fig. 13.

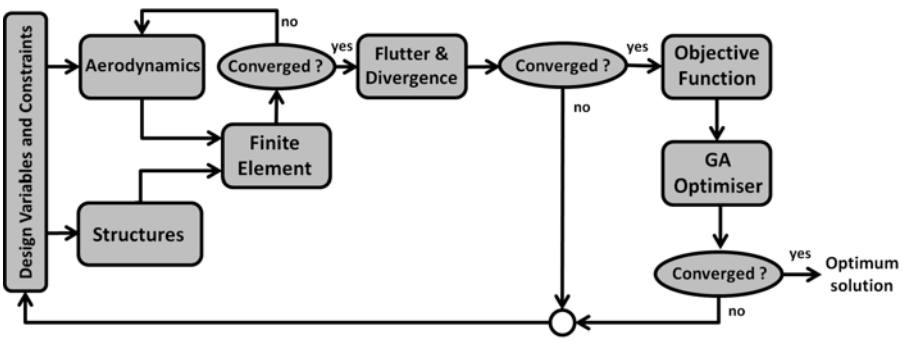

Figure 13. Flowchart and relational diagram of the MDO Suite.

6.2 Genetic Algorithm (GA) optimiser

Genetic Algorithms (GAs) are stochastic global search and optimisation methods. GAs mimic the metaphor of natural evolution by applying the principle of the survival of the fittest to produce successively better approximations to a solution[25]. They follow a population-based approach which allows the optimisation process to be parallelised and hence to reduce the computational time. GAs start with an initial population consisting of various individuals, and each individual represents a particular solution to the problem. The

population evolves over generations to produce better solutions. The 'Matlab GA Toolbox', developed by Chipperfield *et al*[26] was incorporated in this analysis. A fitness value is assigned to every individual of the initial population through an objective function that assesses the performance of the individual in the problem domain. Then, individuals are selected based on their fitness index and crossover between them is performed to generate new offspring. Finally, mutation of the new offspring is performed to ensure that the probability of searching any subspace of the problem is never zero. These abovementioned processes iterate until the optimum solution is achieved depending on the convergence criteria of the problem.

6.3 Optimum roll control

For the ATW to be a successful roll device it must provide the required rolling moment throughout the entire mission profile of the UAV. As stressed above, roll control is achieved by changing the web locations on one side of the wing only. The aeroelastic twist induced increases the lift on one side of the wing leading to a large rolling moment. At the start of cruise, an aileron deflection of 5° generates a rolling moment (RM) of L = 8kNm and a yawing moment (YM) of N = 745Nm, resulting in an RM to YM ratio of 10·74. The objective in this study is to achieve at least the same rolling moment while maximising the ratio of RM to YM (rolling efficiency factor). The MDO suite is employed and the optimisation problem is summarised in Table 2.

A GA run of 50 generations with 100 individuals has been selected. A rolling moment of L = 8kNm and a yawing moment N = 478Nm were achieved. This resulted in an RM to YM ratio of 16·73. For a symmetric aileron deflection to achieve the same rolling moment resulted in a RM to YW ratio of 10·74. This indicates that the ATW provides a more useful rolling device as it can minimise the associated adverse yawing moment by up to 35%, which would result in much lower drag overall especially at low speed flight phases where induced drag is dominant. The optimum web configuration from the GA is listed in Table 3.

A tip twist of 2·1° was achieved. It should be noted that the optimiser moves both webs as close as possible to the maximum permissible value in partition 1 at the wing root. Furthermore, the optimiser minimises the movement of the spar webs in partitions 2, 3, 4, and 5. Figure 14 shows the spanwise aeroelastic twist. The change in aeroelastic twist is the largest over partition 1 and then it settles down and starts to drop gradually until it becomes negligible over partition 5. Therefore to maximise the RM to YM ratio, the optimiser shifts the lift distribution (maximum aeroelastic twist) inboard although this results in a smaller

Table 2
Roll control optimisation problem without root constraint

Objective	**Maximise (L /N)**	
Variables	x_{1_i} x_{2_i} i = 1, 2, ...,5	
Constraints	$0\% \le x_{1_i} \le 40\%$ $0\% \le x_{2_i} \le 40\%$ $x_{1_i} + x_{2_i} \le 70\%$ $8\text{kNm} \le L \le 10\text{kNm}$	$N \le 745\text{Nm}$ altitude = 10,000ft $V_d \le 1{\cdot}25V_{dd}$ $V_F \le 1{\cdot}25V_{dd}$

Table 3
Optimum positions without root constraints

Webs	P1	P2	P3	P4	P5
Front	39	4	0	0	0
Rear	31	0	0	0	0

moment arm and smaller adverse yawing moment. By examining the optimum web positions, the optimiser minimises the torsional stiffness as much as possible around the root section. In practice, this is difficult to achieve due to the various functions of the wing root and the conflicting design requirements, in addition the flutter and divergence speeds reduce. Therefore to minimise the movement of the webs in the wing root partition, a new constraint is added yielding a new optimisation problem summarised in Table 4.

A GA run of 50 generations with 100 individuals has been selected. An RM to YM ratio of 14·95 was achieved. A rolling moment L_r = 8kNm and a yawing moment of N = 535Nm were achieved. The adverse yawing moment has reduced by 28%. A tip twist of 2·4° was achieved. The optimum web configurations from the GA are listed in Table 5.

The optimiser drives the webs in partitions 1 and 2 to the maximum permissible value. For partitions 3 and 4 the optimiser drives the front web rearward and keeps the rear fixed in its original position, while it fixes both webs in their original positions for partition 5. Figure 14 shows the spanwise aeroelastic twist to maximise the RM to YM ratio where the movement of the webs in partition 1 is constrained. The largest change in the twist occurs over partition 2, and then the rate of twist starts to settle down and becomes almost zero over partition 5. The tip twist achieved with the root constraint is higher than the case without constraint. Furthermore the lift distribution is shifted outboard when compared to the case where there is no constraint.

Table 4
Roll control optimisation problem with root constraint

Objective	**Maximise (L/N)**	
Variables	x_{1_i} x_{2_i} i = 1, 2, ...,5	
Constraints	$0\% \le x_{1_i} \le 40\%$ $0\% \le x_{2_i} \le 40\%$ $x_{1_i} + x_{2_i} \le 70\%$ $x_{1_i} \le 20\%$ $x_{2_i} \le 20\%$	8kNm $\le L \le$ 10kNm $N \le$ 745Nm altitude = 10,000ft $V_d \le 1{\cdot}25V_{dd}$ $V_F \le 1{\cdot}25V_{dd}$

Table 5
Optimum positions with root constraints

Webs	P1	P2	P3	P4	P5
Front	39	4	0	0	0
Rear	31	0	0	0	0

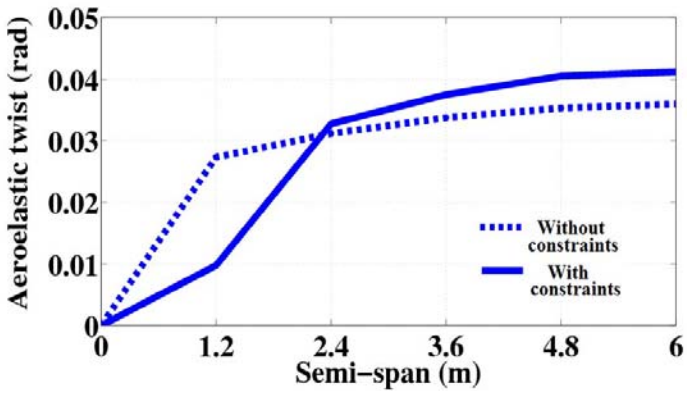

Figure 14. Spanwise aeroelastic twist to maximise rolling efficiency.

7.0 POTENTIAL IMPLEMENTATION

Figure 15 shows the rectangular cross-section ATW embedded inside the aerofoil. The heights of the front and rear spar webs are identical and equal to 8% of the wing chord. Hexagonal aluminium honeycomb covered by an elastomeric skin surrounds the ATW in order to maintain the profile of the aerofoil and to transfer the aerodynamics loads to the ATW. The ATW carries the majority of the loads and has all the functionalities of a conventional wingbox. The webs can translate through the hollowed spar caps using connecting shafts and rolling bearings. Hydraulic actuators are employed to translate the webs and lock them in their new desired positions. The aerodynamic loads are then transferred through the honeycomb to the Aluminium covers of the ATW which carry the majority of the bending and torsional loads. The shear loads are carried mainly by the webs and they are transferred from the covers to the webs through the rolling bearings and connecting shafts.

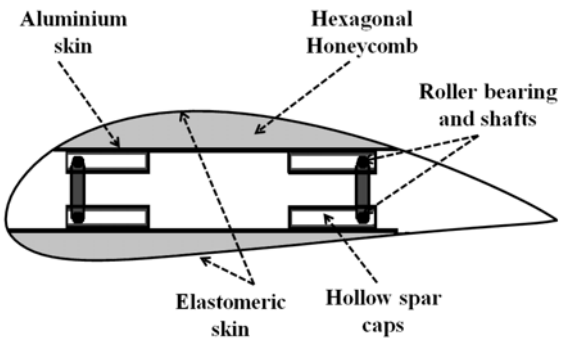

Figure 15. Potential implementation of the ATW.

8.0 CONCLUSIONS

The Adaptive Torsion wing (ATW) concept has been presented. Detailed conceptual modelling of the concept was performed using a conceptual quasi-static aeroelastic suite. A feasibility study to assess the potential benefits of the Adaptive Torsion Wing (ATW) concept was carried out. Preliminary results indicate that significant increase in tip twist and lift force can be achieved by

moving the front spar web. However, this is also associated with large reductions in divergence and flutter speeds. On the other hand, the rear web provides slight increase in tip twist and lift, but minimal drop in divergence and flutter speeds as it moves the shear centre close to the aerodynamic centre. The benefits of the concept can be maximised by a combined movement of the front and rear webs, as the front web provides the aeroelastic twist and the rear web provides a stable aeroelastic structure. Furthermore, the feasibility of using the ATW as a rolling device and to replace conventional ailerons was investigated. The ATW is capable of providing the required rolling moment with smaller induced yawing moment, resulting in a smaller drag penalty when compared to ailerons.

ACKNOWLEDGEMENTS

The authors acknowledge funding from the European Research Council through Grant Number 247045 entitled *Optimisation of Multiscale Structures with Applications to Morphing Aircraft*.

REFERENCES

1. TORENBEEK, E. Development and Application of a Comprehensive, Design-sensitive Weight Prediction Method for Wing Structures of Transport Category Aircr. Delft University of Technology, Report LR-693, 1992.
2. MILLER, G.D. Active Flexible Wing (AFW) Technology, Rockwell International North American Aircr Operations, 1988, Los Angeles, CA, USA, Report: AFWAL-TR-87-3096.
3. CLARKE, R., ALLEN, M.J., DIBLEY, R.P., GERA, J. and HODGKINSON, J. Flight Test of the F/A-18 Active Aeroelastic Wing Airplane, AIAA Atmospheric Flight Mechanics Conference and Exhibit, 2005, San Francisco, CA, USA, AIAA 2005-6316.
4. PENDLETON, E.W., BESSETTE, D., FIELD, P.B., MILLER, G.D. and GRIFFIN, K.E. Active aeroelastic wing flight research program: technical program and model analytical development, *J Aircr*, 2000, **37**, (4), pp 554-561, doi: 10.2514/2.2654.
5. GRIFFIN, K.E. and HOPKINS, M.A. Smart stiffness for improved roll control, *J Aircr*, Engineering notes, 1997, **34**, (3), pp 445-447.
6. CHEN, P.C., SARHADDI, D., JHA, R., LIU, D.D., GRIFFIN, K. and YURKOVICH, R. Variable stiffness spar approach for aircraft manoeuvre enhancement using ASTROS, *J Aircr*, September-October 2000, **37**, (5).
7. NAM, C., CHEN, P.C., SARHADDI, D., LIU, D., GRIFFIN, K. and YURKOVICH, R. Torsion-Free Wing Concept for Aircraft Maneuver Enhancement, AIAA/ASME/ASCE/AHS/ASC Structures, 2000, Structural Dynamics and Materials Conference, Atlanta, GA, USA, AIAA 2000-1620.
8. FLORANCE, J.R., HEEG, J., SPAIN, C.V. and LIVELY, P.S. Variable Stiffness Spar Wind-Tunnel Modal Development azzzzzznd Testing, 45th AIAA/ASME/ASCE/AHS/ASC/ Structures, 2004, Structural Dynamics and Materials Conference, Palm Springs, California, USA, AIAA 2004-1588.
9. KUZMINA, S., AMIRYANTS, G., SCHWEIGER, J., COOPER, J., AMPRIKIDIS, M. and SENSBERG, O. Review and Outlook on Active and Passive Aeroelastic Design Concept for Future Aircraft, ICAS 2002 Congress, 8-13 September, Toronto, Canada, ICAS, **432**, 2002, pp 1–10.
10. SCHWEIGER, J. and SULEMAN, A. The European Research Project – Active Aeroelastic Structures, CEAS Int Forum on Aeroelasticity and Structural Dynamics, 2003.
11. SIMPSON J., ANGUITA-DELGADO L., KAWIESKI G., NILSSON B., VACCARO V. and KAWIECKI, G. Review of European Research Project Active Aeroelastic Aircraft Structures (3AS), European Conference for Aerospace Sciences (EUCASS), 2005, Moscow, Russia.
12. AMPRIKIDIS, M., COOPER, J.E. and SENSBURG, O. Development of an Adaptive Stiffness All-Moving Vertical Tail, 45th AIAA/ASME/ASCE/AHS/ASC Structures, Structural Dynamics and Materials Conference, Palm Spring, California, USA, 2004, AIAA 2004-1883.
13. COOPER, J.E., AMPRIKIDIS, M., AMEDURI, S., CONCILIO, A., SAN MILLAN, J. and CASTANON, M. Adaptive Stiffness Systems for an Active All-Moving Vertical Tail, European Conference for Aerospace Sciences (EUCASS), 4-7th July 2005, Moscow, Russia.

14. COOPER, J.E. Adaptive stiffness structures for air vehicle drag reduction, In Multifunctional Structures/Integration of Sensors and Antennas (pp 15-1-15-12). Meeting Proceedings RTO-MP-AVT-141, Paper 15.Nueuilly-sur-Seine, France: RTO, 2006.
15. COOPER, J.E. Towards the Optimisation of Adaptive Aeroelastic Structures, School of Mechanical, Aerospace and Civil Engineering, University of Manchester, Manchester, UK, 2006.
16. HODIGERE-SIDDARAMAIAH, V. and COOPER, J.E. On the Use of Adaptive Internal Structures to Optimise Wing Aerodynamics Distribution, 47th AIAA/ASME/ASCE/AHS/ASC Structures, 2006, Structural Dynamics and Materials Conference, Newport, Rhode Island, USA, AIAA 2006-2131.
17. AJAJ, R.M., FRISWELL, M.I., DETTMER, W.G., ALLEGRI, G. and ISIKVEREN, A.T. Conceptual Modelling of an Adaptive Torsion Structure, 52nd AIAA/ASME/ASCE/AHS/ASC Structures, Structural Dynamics and Materials Conference, Denver, Colorado, USA, AIAA-2011-1883, 2011.
18. AJAJ, R.M., FRISWELL, M.I., DETTMER, W.G., ALLEGRI, G. and ISIKVEREN, A.T. Roll Control of a UAV Using an Adaptive Torsion Structure, 52nd AIAA/ASME/ASCE/AHS/ASC Structures, Structural Dynamics and Materials Conference, Denver, Colorado, USA, AIAA-2011-1883, 2011.
19. AJAJ, R.M., FRISWELL, M.I., DETTMER, W.G., ALLEGRI G. and ISIKVEREN, A.T. 2012. Dynamic Modelling and Actuation of the Adaptive Torsion Wing, *J Intelligent Material Systems and Structures*, doi: 10.1177/1045389X12444493.
20. MELIN, T. A Vortex Lattice MATLAB Implementation for Linear Aerodynamic Wing Applications. Master's Thesis, Royal Institute of Technology (KTH), Department of Aeronautics, Sweden, 2000.
21. MELIN, T. User's guide and reference manual for Tornado, Royal Institute of Technology (KTH), Department of Aeronautics, Sweden, 2000.
22. MEGSON, T.H.G. *Aircraft Structures for Engineering Students*, New York: Butterworth-Heinemann, 2003.
23. WRIGHT, J.R. and COOPER, J.E. *Introduction to Aircraft Aeroelasticity and Loads*, **11**, Dynamic Aeroelasticity-Flutter, John Wiley & Sons Ltd, 2007.
24. BRUNTON, S.L. and ROWLEY, C.W. Low-dimensional State-Space Representations for Classical Unsteady Aerodynamic Models, 49th AIAA Aerospace Sciences Meeting including the New Horizons Forum and Aerospace Exposition, Orlando, Florida, USA, 2011, AIAA-2011-476.